Draft for NIMA
version 4.1
August 13, 2015

Separating double-beta decay events from solar neutrino interactions in kiloton-scale liquid scintillator detectors

Andrey Elagin[1], Henry Frisch[1], Lindley Winslow[2], *et al* **(opt-in)**
[1]*Enrico Fermi Institute, University of Chicago*
[2]*Massachusetts Institute of Technology*

Abstract

We propose a technique for separating $0\nu\beta\beta$-decay events from background due to ^8B solar neutrino interactions in a liquid scintillator detector. The technique compares event topology of the signal and background events using spherical harmonics analysis of the early light emitted in $0\nu\beta\beta$-decay and ^8B events. Selection of early photons using fast photo-detectors allows for separation of directional Cherenkov from isotropic scintillation light and identification of two event topologies based on the spatial distribution of the early photons in the detector.

Contents

1 Introduction

Introductory paragraph saying that $0\nu\beta\beta$-decay is important and we'd like to improve sensitivity of liquid scintillator detectors.

Another paragraph saying that this is a follow up on our preceding paper [1]

As have been shown in [1] photo-detectors with time resolution of ∼100 ps can allow for selection of photons that contain significant fraction of Cherenkov light produced by 1-5 MeV electrons in a kilo-ton scale liquid scintillator detector.

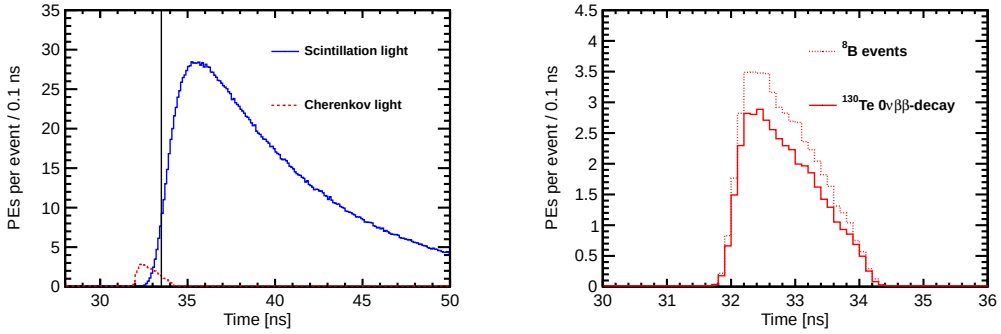

Figure 1: (Left) Photo-electron (PE) arrival times after application of the photo-detector transit time spread (TTS) of 100 ps for the simulation of 1000 $0\nu\beta\beta$-decay events of ^{130}Te at the center of the detector. PEs from Cherenkov light (red, dash line) and scintillation light (blue, solid line) are compared. The black vertical line illustrates a time cut at 33.5 ns. (Right) Comparison between Cherenkov PEs arrival time for ^{130}Te $0\nu\beta\beta$-decay (solid line) and ^{8}B (dotted line) events. **Distributions of the scintillation PEs arrival time are indistinguishable between ^{130}Te $0\nu\beta\beta$-decay and ^{8}B due to identical total energy in the event, Q(^{130}Te)=2.529 MeV.**

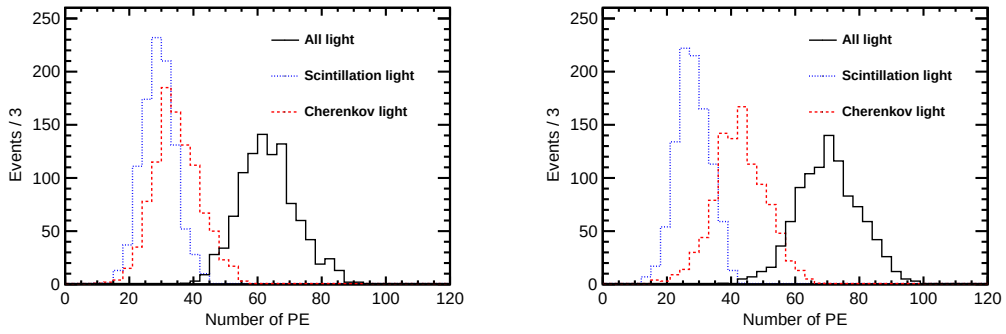

Figure 2: Number of Cherenkov (red dash line), scintillation (blue dotted line), and total (black solid line) PEs for the simulatio of 1000 ^{130}Te $0\nu\beta\beta$-decay (left panel) and ^{8}B (right panel) events.

2 Discussion on backgrounds

In a large liquid scintillator detector two dominant backgrounds to $0\nu\beta\beta$-decay signal are $2\nu\beta\beta$-decay and QE interactions of ^{8}B solar neutrinos. As an example we show comparison between signal and various backgrounds for SNO+ experiment in Fig. 3.

Figure 4 shows kinematics of $0\nu\beta\beta$- and $2\nu\beta\beta$-decays. In the region of interest (ROI) where total kinetic energy of the electrons is close to the energy spectrum end point, Q-value, there is no difference in kinematics of $0\nu\beta\beta$- and $2\nu\beta\beta$-decays. Therefore the energy resolution is the key detector parameter to discriminate between $0\nu\beta\beta$- and $2\nu\beta\beta$-decays.

While the $2\nu\beta\beta$-decay is topologically very similar to the $0\nu\beta\beta$-decay signal the next largest background coming from the ^{8}B solar neutrino interactions result in one electron that leads to a distinct pattern of the Cherenkov photons.

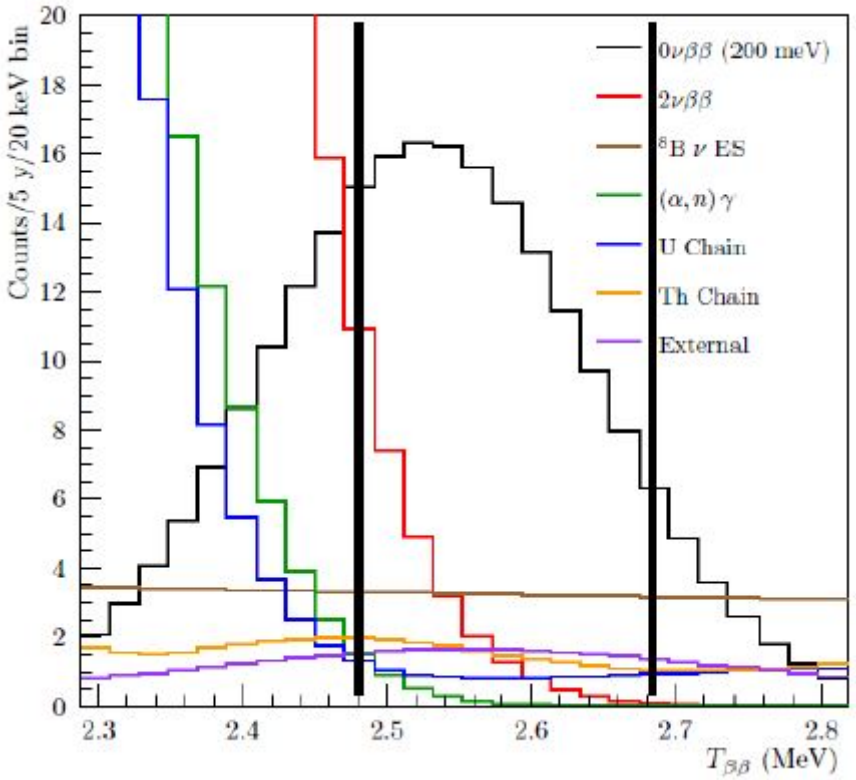

Figure 3: SNO+ Phase I signal and background energy spectrum (visible kinetic energy reconstructed under a $0\nu\beta\beta$ hypothesis). Plot taken from [2]

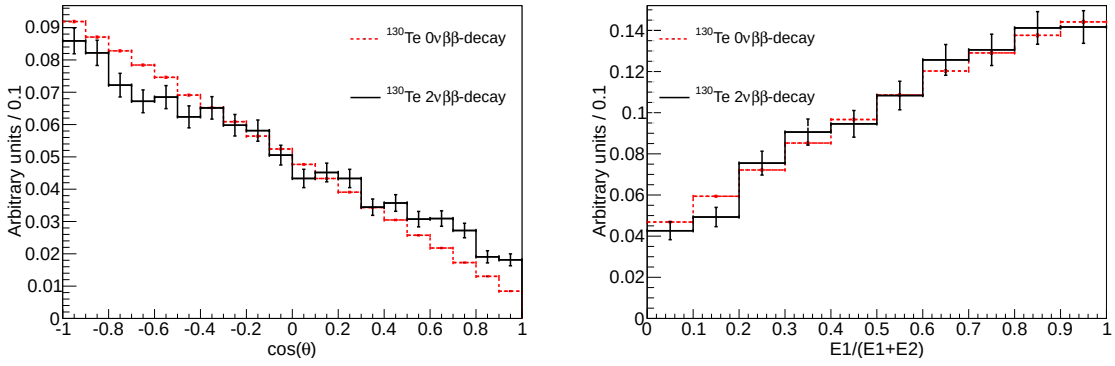

Figure 4: Comparison between kinematics of $0\nu\beta\beta$- (dashed red lines) and $2\nu\beta\beta$-decays (solid black lines) for events with the total kinetic energy of the electrons above 90% of the Q-value. (Left) Cosine of the angle between two electrons. (Right) Fraction of energy carried by one of the two electrons. Due to limited statistic around the energy spectrum end point for $2\nu\beta\beta$-decay we show statistical errors for each bin.

3 Description of the detector geometry and simulation

Details are in [1]. Only one or two paragraphs here.

4 Event Topology and Spherical Harmonics

Signature of the $0\nu\beta\beta$-decay is two electrons with total kinetic energy equal to the isotope Q-value (e.g., 2.529 MeV for ^{130}Te). These two electrons are often above Cherenkov threshold and therefore will produce two (fuzzy) rings of Cherenkov light on top of isotropic scintillation light. ^{8}B background events have only one electron producing one Cherenkov ring.

In the detector regions where Cherenkov and scintillation light overlap the Cherenkov light on average arrives earlier due to a time delay in emission and a shorter wavelengths of the scintillation light. Therefore, while a vast majority of light produced in $0\nu\beta\beta$-decay events consists of scintillation photons, timing information can be used to select a sample of photons with high fraction of Cherenkov light.

Due to directional nature of the Cherenkov light the spatial distribution of early photons on the detector sphere will be different for the $0\nu\beta\beta$-decay signal and the background from ^{8}B events. Figure 5 shows event displays of ^{130}Te $0\nu\beta\beta$-decay signal events and ^{8}B background. For quantitative description of the difference in the event topology we analyze spherical harmonics of the photon distributions on the detector sphere. We construct rotation invariant variables and compare them between signal and background events.

The simplest case for spherical harmonics analysis are events with the vertex located exactly in the center of the detector. For such event Cherenkov and scintillation light can be separated by applying a time cut on the photon arrival time as demonstrated in [1]. To introduce the technique of spherical harmonics analysis we will follow the same strategy as in [1] and use central events with a slightly different cut on the photon

arrival time of 33.5 ns.

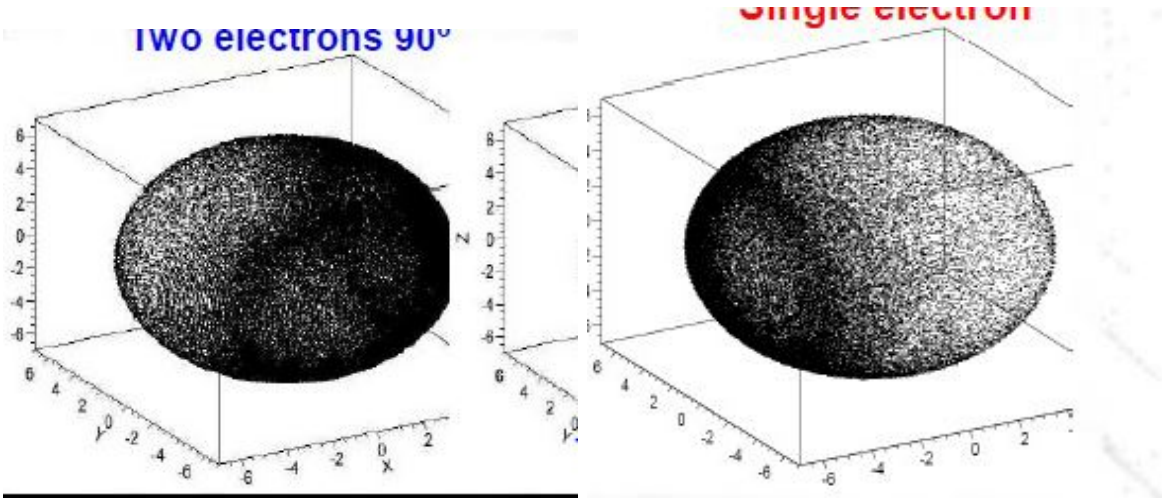

Figure 5: Examples of PEs position on the detector sphere after time cut of 33.5ns. PEs from Cherenkov (red) and scintillation light (blue) are compared. (Left) PEs from two electrons produced in an event of $0\nu\beta\beta$-decay of ^{130}Te. In this event the angle between the electrons is $\sim 90^o$ and the electrons energies are A.B MeV and D.C MeV. (Right) PEs from one electron produced in an event of ^8B solar neutrino interaction. In this event the electron energy is E.F MeV.

4.1 Mathematical description of spherical harmonics analysis

A function $f(\theta, \phi)$ can be decomposed to a sum of spherical harmonics:

$$f(\theta, \phi) = \sum_{l=0}^{\infty} \sum_{m=-l}^{l} f_{lm} Y_{lm}(\theta, \phi), \tag{1}$$

where Y_{lm} are Laplace's spherical harmonics defined in Eq. 2 in real-value basis using Legendre polynomials P_l. Coefficients f_{lm} are defined in Eq. 3

$$Y_{lm} = LONG formula HERE \tag{2}$$

$$f_{lm} = LONG formula HERE \tag{3}$$

Equation 4 defines multiple moments S_l which are invariant under rotation. Combination of S_l's for (l=0,1,2...) is determined by the event topology and can be used to distinguish between different topologies.

$$S_l = \sum_{m=-l}^{m=l} |f_{lm}|^2 \tag{4}$$

Figure 6 compares S_l distributions for two electrons emitted at 180 degree, two electrons at 90 degree, and a single electron. Total kinetic energy of the electrons is the same in all three cases.

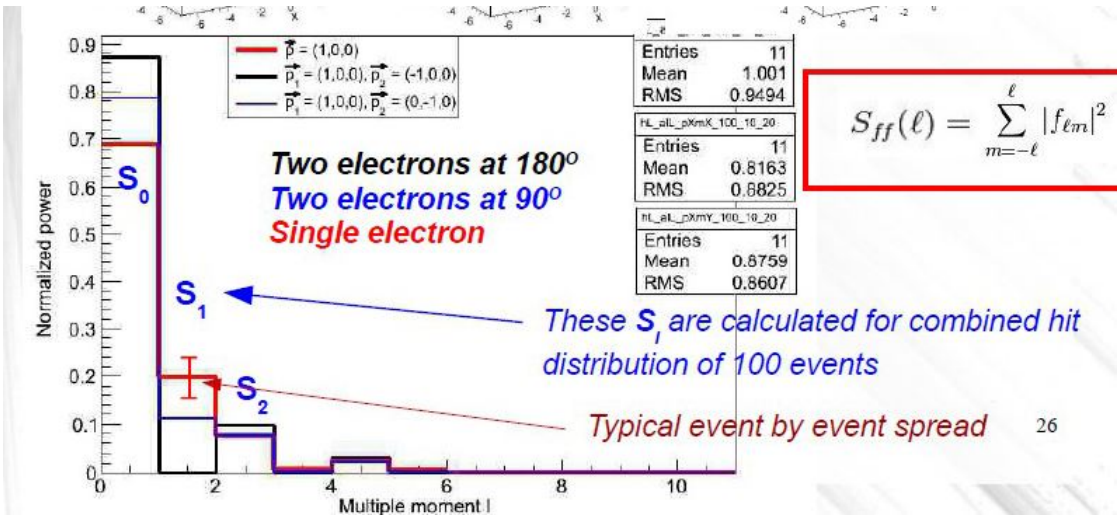

Figure 6: Average S_l values for two electrons at 180 degree (color1) and 90 degree (color2) 1.5 MeV each and a single electron (color3) with the energy of 3 MeV. Error bars are RMS values of each corresponding individual S_l distribution (each consists of 1000 events simulated at the center of the detector) indicating typical event-by-event variation.

In order to compare spherical harmonics for events with vertices located off-center anywhere inside the detector volume a coordinate transformation for each photon hit

is needed. The transformation applied for each photon hit within an event is shown in Fig. 7. Solid circle schematically shows actual detector boundaries. Dotted circle shows a new sphere of radius R=6.5 m with the event vertex position in the center. The radius vector of each photon hit is stretched or shorten until intersection with this new sphere using transformation $\vec{r}_{hit} = \frac{\vec{a}}{|\vec{a}|} \cdot R$. Where $\vec{r}_{hit}$ is a new radius vector of the photon hit, R is detector sphere radius, and $\vec{a} = \vec{r}_{hit} - \vec{r}_{vtx}$ with $\vec{r}_{hit}$ and $\vec{r}_{vtx}$ being radius vectors of the photon hit and vertex position in original coordinates.

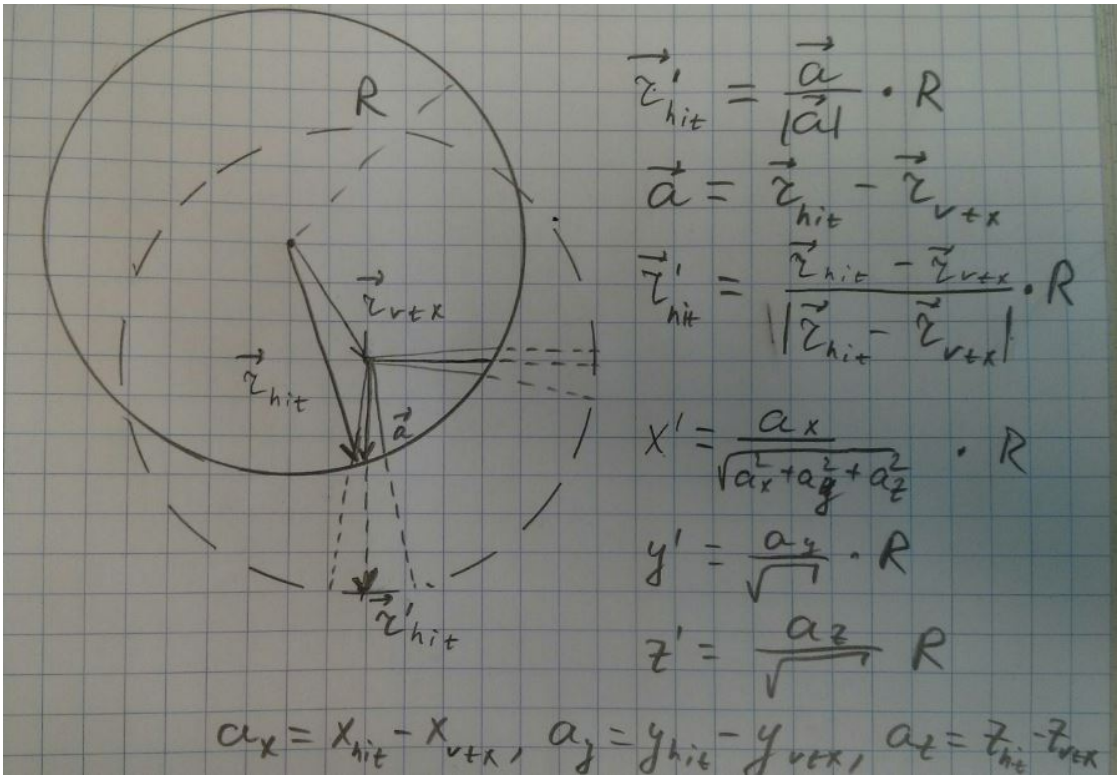

Figure 7: Coordinate transformation applied to events that are off-center. Solid circle schematically shows actual detector boundaries. Dotted circle shows a new sphere of radius R=6.5 m with the event vertex position in the center. The radius vector of each photon hit is stretched or shorten until intersection with this new sphere using transformation $\vec{r}_{hit} = \frac{\vec{a}}{|\vec{a}|} \cdot R$. Where $\vec{r}_{hit}$ is a new radius vector of the photon hit, R is detector sphere radius, and $\vec{a} = \vec{r}_{hit} - \vec{r}_{vtx}$ with $\vec{r}_{hit}$ and $\vec{r}_{vtx}$ being radius vectors of the photon hit and vertex position in original coordinates and correspondingly.

4.2 Software and implementation of the spherical harmonics analysis

A few words on the implementation. Calculation of S_l's requires numerical integration that needs to be explained.

4.3 Performance of the spherical harmonics analysis on $0\nu\beta\beta$-decay and ^8B events.

Comparison of S_0 and S_1 distributions between $0\nu\beta\beta$-decay and ^8B events is shown in Fig. 8. There is a noticeable separation between the signal and background. We also note that in the energy range of interest S_l's do not have strong dependence on the energy deposited in the detector, which makes them reliable discriminators at the end point of the $0\nu\beta\beta$-decay energy spectrum. The information about the event topology is complimentary to the energy measurements.

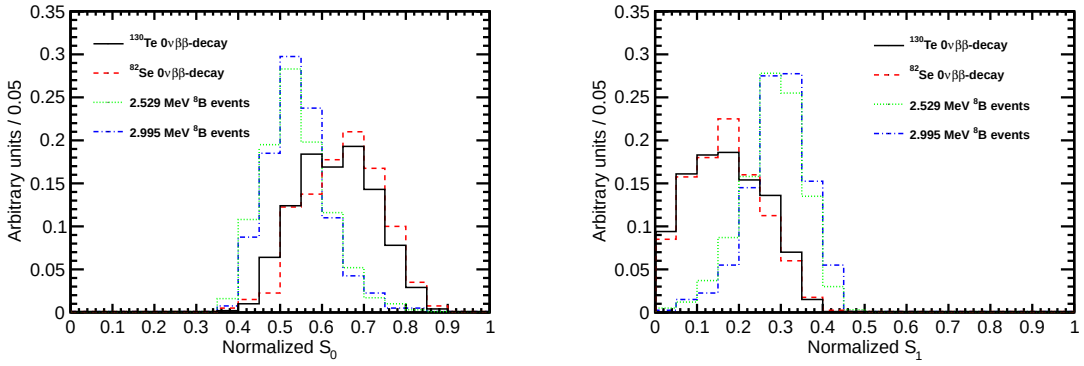

Figure 8: S_0 (left) and S_1 (right) distributions for events with two different event topologies and total kinetic energy. ^{130}Te, ^{82}Se $0\nu\beta\beta$-decay, 2.529 MeV and 2.995 MeV events are compared. The simulation is done for events with the vertex in the center of the detector. ^8B events are implemented as 2.529 MeV or 2.995 MeV electrons with initial direction along x-axis. Perfect vertex reconstruction - true vertex position is used. Time cut of 33.5 ns on the photon arrival time is applied.

Figure 9 shows separation between ^{130}Te signal and ^8B background events simulated at the center of the detector. True values of vertex position and time is used. Time cut

of 33.5 ns on the photon arrival time is applied to separate Cherenkov and scintillation light. **See caption for detail on S_{01} variable.**

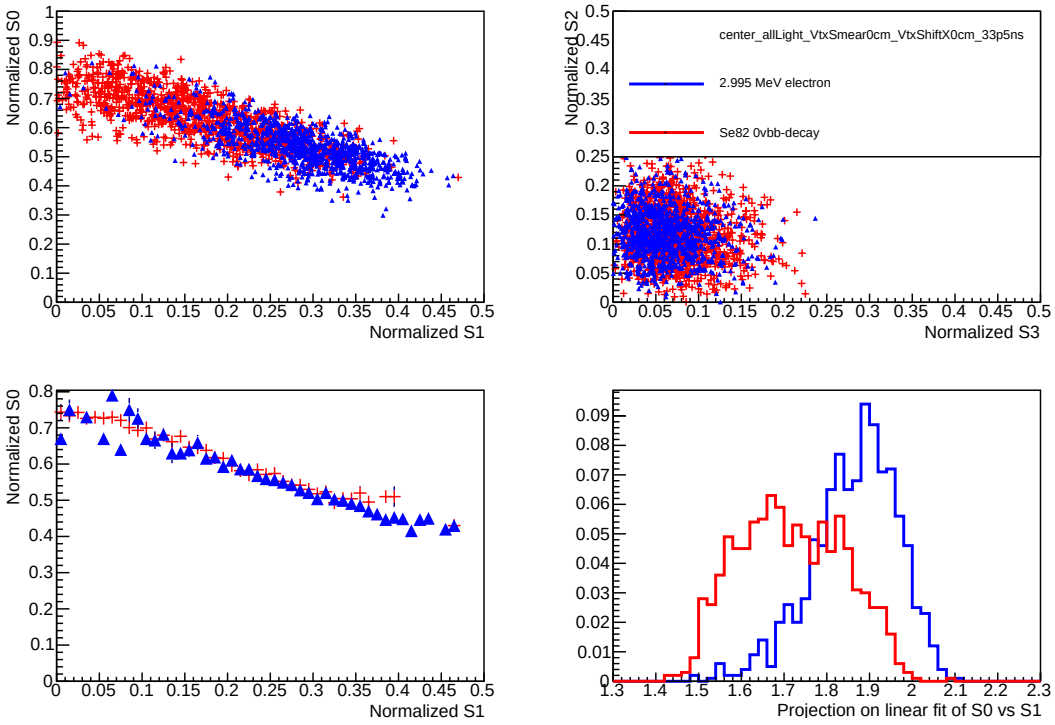

Figure 9: Spherical harmonics comparison between ^{130}Te $0\nu\beta\beta$-decay signal (Q=2.529 MeV) (red) and ^{8}B solar neutrinos background (blue) for 1000 simulated events originated at the center of the sphere. ^{8}B events are implemented as 2.529 MeV electrons with initial direction along x-axis. Perfect vertex reconstruction - true vertex position is used. Time cut of 33.5 ns on the photon arrival time is applied. (Top left) S_0 versus S_1 scatter plot. (Top right) S_2 versus S_3 scatter plot (shown for completeness - no significant separation power, this canvas space is temporarily used for the legend). (Bottom left) X-profile histogram of the S_0 versus S_1 scatter plot. A linear fit ($S_0 = a \cdot S_1 + b$) is done on this profile histogram to define a 1-dimensional variable $S_{01}=S_1-a \cdot S_0-b$ that provides a better separation between the signal and background. (Bottom right) Distribution of the S_{01} variable calculated for signal (red) and background (blue).

5 Experimental challenges

So far only events at the center of the detector have been considered. In this section we discuss performance of the spherical harmonics analysis for events distributed

within the fiducial volume of the detector taking into account finite resolution on vertex position reconstruction.

When the vertex is not at the center, a uniform time cut on the photon arrival time is no longer effective in the selection of Cherenkov photons. In the case of off-center vertex, even significantly delayed scintillation photons can reach the side of the detector that is closer to the vertex much earlier than Cherenkov photons traveling to the opposite side of the detector. Therefore, the time cut has to be position dependent and take into account the total distance traveled by each individual photon.

We found that the time cut defined as $\Delta t = t^{phot}_{measured} - t^{phot}_{predicted} < 1$ ns selects photons with sufficient fraction of Cherenkov photons. Predicted time, $t^{phot}_{predicted} = l/v^{phot}$, depends on total distance, l, traveled by the photon and proper assignment of the velocity for each photon, v^{phot}, that depends on index of refraction[1]. Therefore the relative Cherenkov/scintillation composition of the light selected with this Δt time cut depends on the vertex location and chromatic dispersions.

Due to chromatic dispersion, even with perfect vertex reconstruction one cannot achieve the same level of separation between Chrerenkov and scintillation light compared to the central events considered above in Section 4. This in turn reduces the effectiveness of the spherical harmonics analysis in separating of $0\nu\beta\beta$-decay and ^8B events (see Fig. 10). However next generation detectors can recover losses due to chromatic dispersion by choosing liquid scintillators with a more narrow emission spectrum.

Imprecise knowledge of the vertex position due to finite resolution is another factor affecting performance of the spherical harmonics analysis. Small deviations in vertex reconstruction cause large effect on S_0 and S_1 for single electron event topology. For the verticies shifted along the direction of the electron the Δt cut makes uniform scintillation light distribution less uniform. The Δt cut selects more forward emitted photons in the case when the reconstructed vertex is shifted to the direction opposite to the electron momentum (enhancing forward region populated by Cherenkov photons - more asymmetric photon distribution causing higher values of S_1). It selects more

[1]We use average index of refraction of n=1.53

backward emitted photons in the case when the reconstructed vertex is shifted in the direction along the electron momentum (counter balancing forward region populated by Cherenkov photons - more symmetric photon distribution causing smaller values of S_1).

Solution to this problem would be a better selection criteria of early light. It has to preserve high admixture of the Cherenkov photons, but needs to select scintillation photons in a more uniform manner. Working on it, but may not be simple so I don't want to include it in this paper.

Good vertex resolution is essential for spherical harmonics analysis. Such strong dependence on the vertex resolution can be addressed by choosing a different liquid scintillator mixture with a more delayed emission of the scintillation light. Figure 12 shows spherical harmonics calculated for the time profile which has scintillation component delayed by 0.5ns with respect to what is shown in Fig. 1

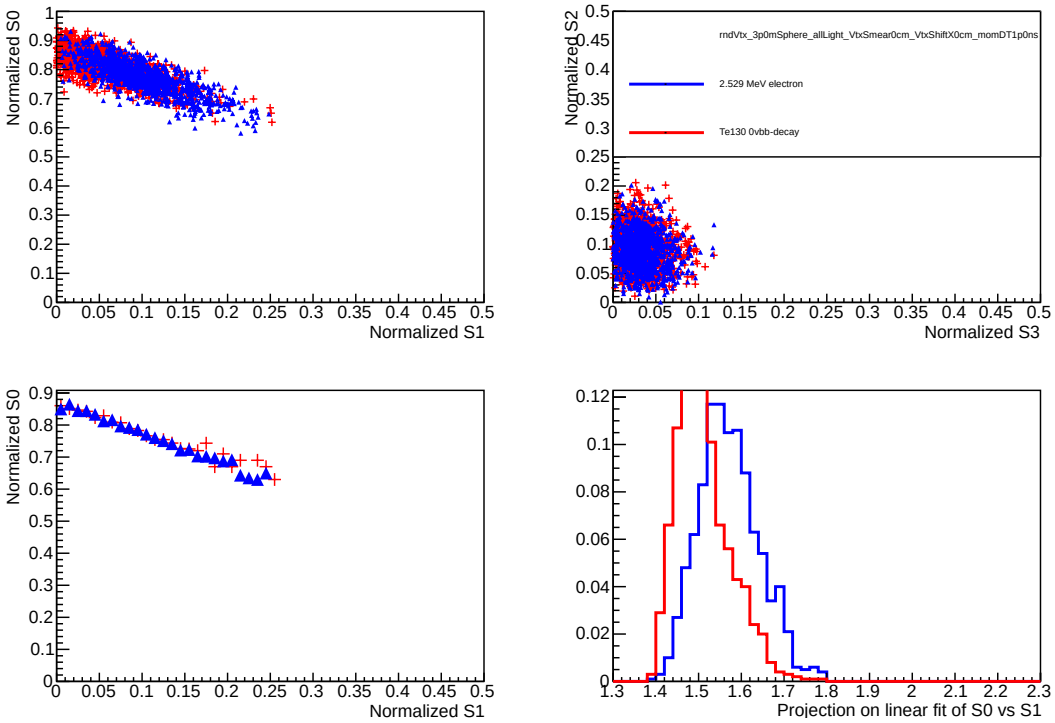

Figure 10: Spherical harmonics comparison between ^{130}Te $0\nu\beta\beta$-decay signal (Q=2.529 MeV) (red) and ^{8}B solar neutrinos background (blue) for 1000 simulated events.Verticies are uniformly distributed within the fiducial volume, R<3 m. ^{8}Be events are implemented as 2.529 MeV electrons with the initial momentum direction uniformly distributed within 4π solid angle. Perfect vertex reconstruction - true vertex position is used. (Top left) S_0 versus S_1 scatter plot. (Top right) S_2 versus S_3 scatter plot (shown for completeness - no significant separation power, this canvas space is temporarily used for the legend). (Bottom left) X-profile histogram of the S_0 versus S_1 scatter plot. A linear fit ($S_0 = a{\cdot}S_1 + b$) is done on this profile histogram to define a 1-dimensional variable S_{01}=S_1-a·S_0-b that provides a better separation between the signal and background. (Bottom right) Distribution of the S_{01} variable calculated for signal (red) and background (blue).

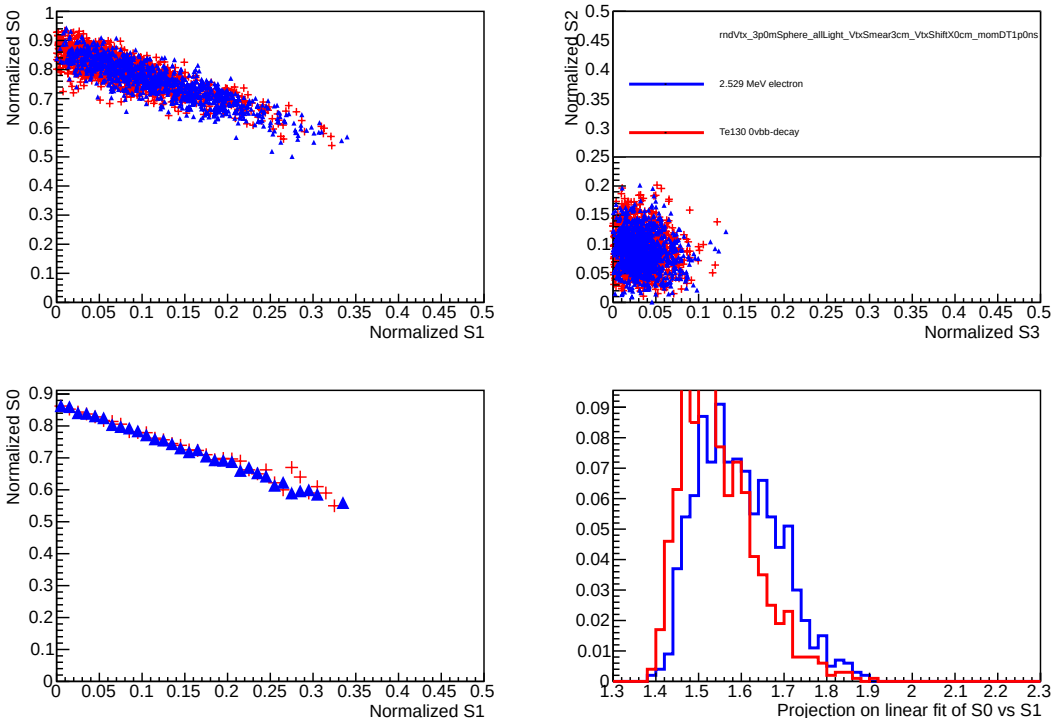

Figure 11: Spherical harmonics comparison between ^{130}Te $0\nu\beta\beta$-decay signal (Q=2.529 MeV) (red) and ^{8}B solar neutrinos background (blue) for 1000 simulated events.Verticies are uniformly distributed within the fiducial volume, R<3 m. ^{8}Be events are implemented as 2.529 MeV electrons with the initial momentum direction uniformly distributed within 4π solid angle. Vetrex is smeared with 3 cm resolution. (Top left) S_0 versus S_1 scatter plot. (Top right) S_2 versus S_3 scatter plot (shown for completeness - no significant separation power, this canvas space is temporarily used for the legend). (Bottom left) X-profile histogram of the S_0 versus S_1 scatter plot. A linear fit ($S_0 = a \cdot S_1 + b$) is done on this profile histogram to define a 1-dimensional variable S_{01}=S_1-a·S_0-b that provides a better separation between the signal and background. (Bottom right) Distribution of the S_{01} variable calculated for signal (red) and background (blue).

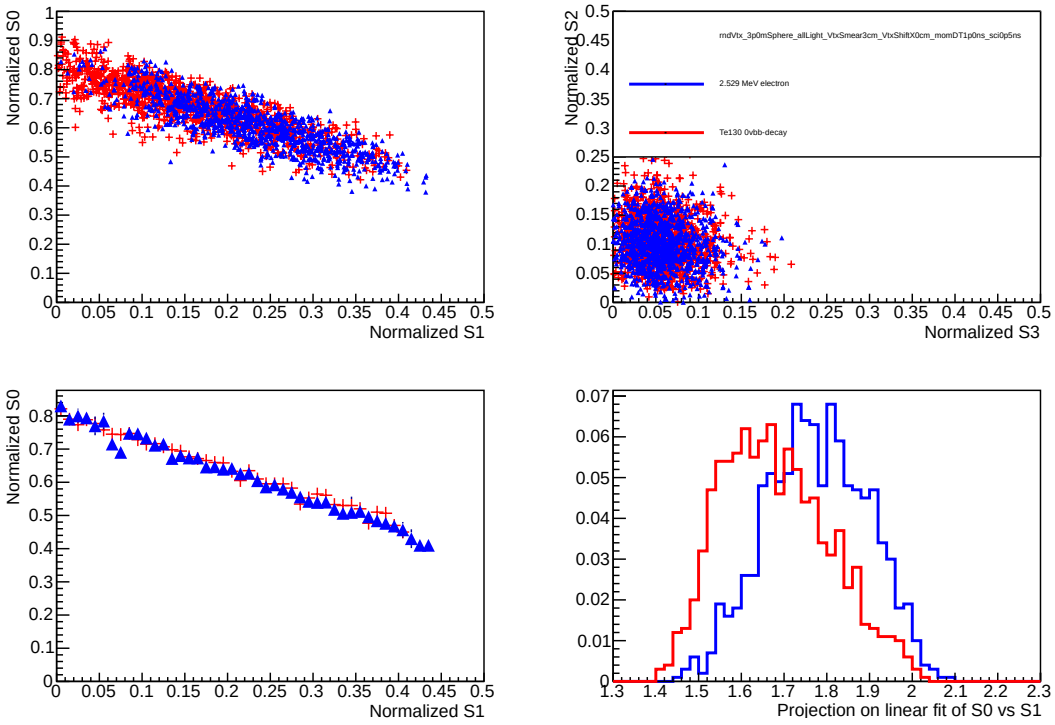

Figure 12: Spherical harmonics comparison between ^{130}Te $0\nu\beta\beta$-decay signal (Q=2.529 MeV) (red) and ^{8}B solar neutrinos background (blue) for 1000 simulated events.Verticies are uniformly distributed within the fiducial volume, R<3 m. ^{8}Be events are implemented as 2.529 MeV electrons with the initial momentum direction uniformly distributed within 4π solid angle. Vetrex is smeared with 3 cm resolution. **Scintillation light is delayed by additional 0.5 ns.** (Top left) S_0 versus S_1 scatter plot. (Top right) S_2 versus S_3 scatter plot (shown for completeness - no significant separation power, this canvas space is temporarily used for the legend). (Bottom left) X-profile histogram of the S_0 versus S_1 scatter plot. A linear fit ($S_0 = a \cdot S_1 + b$) is done on this profile histogram to define a 1-dimensional variable S_{01}=S_1-a·S_0-b that provides a better separation between the signal and background. (Bottom right) Distribution of the S_{01} variable calculated for signal (red) and background (blue).

6 Conclusions

A technique based on spherical harmonics analysis is discussed to separate $0\nu\beta\beta$-decay from ^8B solar neutrino interactions. The separation is based on distinct event topologies of signal and background. This event topology information is available in addition to the measurements of the energy deposited in the detector. This technique may be further developed and adopted by future large scale liquid scintillator detectors to suppress background coming from ^8B solar neutrino interactions in the detector volume. The performance of the technique is mostly affected by chromatic dispersions, vertex reconstruction and time profile of the emission of the scintillation light. We show that a liquid scintillator detector with a $\sim$1 ns total delay of the scintillation light with respect to the Cherenkov light allows for use of spherical harmonics analysis as an extra handle to extract $0\nu\beta\beta$-decay signal.

7 Acknowledgments

To be finalized based on opt-in for the author list.

A $0\nu\beta\beta$-decay vs ^{10}C background

Other common backgrounds to $0\nu\beta\beta$-decay search include radioactive decays of nuclei excited by cosmic muons and decays of Th and U naturally present in the materials. In a liquid scintillator detectors most of events from Th and U decays are happening in the materials of the scintillator enclosure. Typically they enter the fiducial volume as 2.6 MeV gammas. These gammas either shower too late or have mis-reconstructed vertex. Both effects depend on details of a particular experiment and therefore in this paper we make no attempt to introduce a topology reconstruction for the backgrounds coming from Th and U lines. Cosmic induced backgrounds, to the contrary, are more generic and originate inside the fiducial volume. In this section we discuss

event topology of ^{10}C events that are most relevant in the energy of 2-3 MeV.

Typical energy deposition by ^{10}C events is shown in Fig. 13. We propose to use spherical harmonics analysis to separate $0\nu\beta\beta$-decay events from ^{10}C events that within energy resolution overlap with the $0\nu\beta\beta$-decay Q-value.

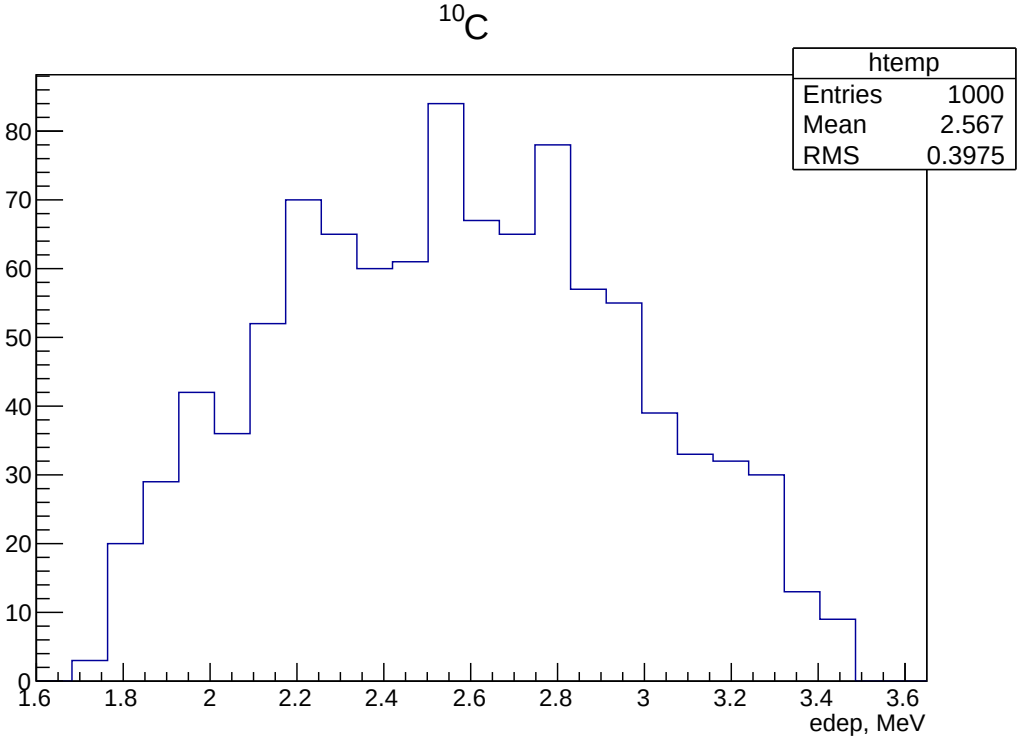

Figure 13: Energy deposition in ^{10}C events.

We note that 98% of ^{10}C decays through the excited state of $^{10}B(718)$ that has a half-life time of $\sim$1 ns. Therefore majority of ^{10}C events have a prompt positron accompanied by a delayed 0.718 MeV gamma. This delayed gamma affects PEs arrival time distribution. Figure 14 shows shape comparison of PEs arrival time distribution between ^{130}Te $0\nu\beta\beta$-decay and ^{10}C events. Time profile of the scintillation photons can be used to separate signal from ^{10}C events.

Comparison of spherical harmonics is shown in Fig. 15. ^{10}C events are generated at the center of the detector. True vertex position is used to apply a 33.5 ns time cut to select photons for the spherical harmonics analysis. The separation is seen in S0 vs S1

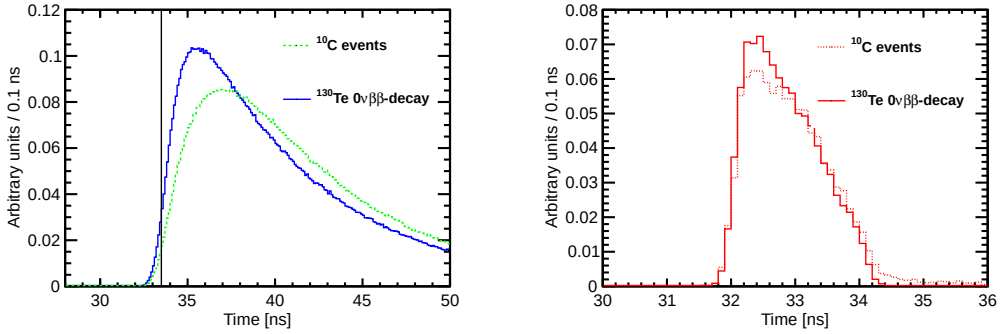

Figure 14: Photo-electron (PE) arrival times after application of the photo-detector transit time spread (TTS) of 100 ps for the simulation of 1000 $0\nu\beta\beta$-decay events of ^{130}Te (solid lines) and ^{10}C (dotted lines) events at the center of the detector. All distributions are normalized for shape comparison. **Absolute number of PEs per event depends on the total energy deposited in the detector. Figure 13 shows energy deposited in the detector in ^{10}C events.** (Left) Scintillation PEs arrival time. The black vertical line illustrates a time cut at 33.5 ns. (Right) Cherenkov PEs arrival time.

and S2 vs S3 scatter plots. We project both scatter plots to a line that gives maximum separation (two bottom panels in Fig. 15).

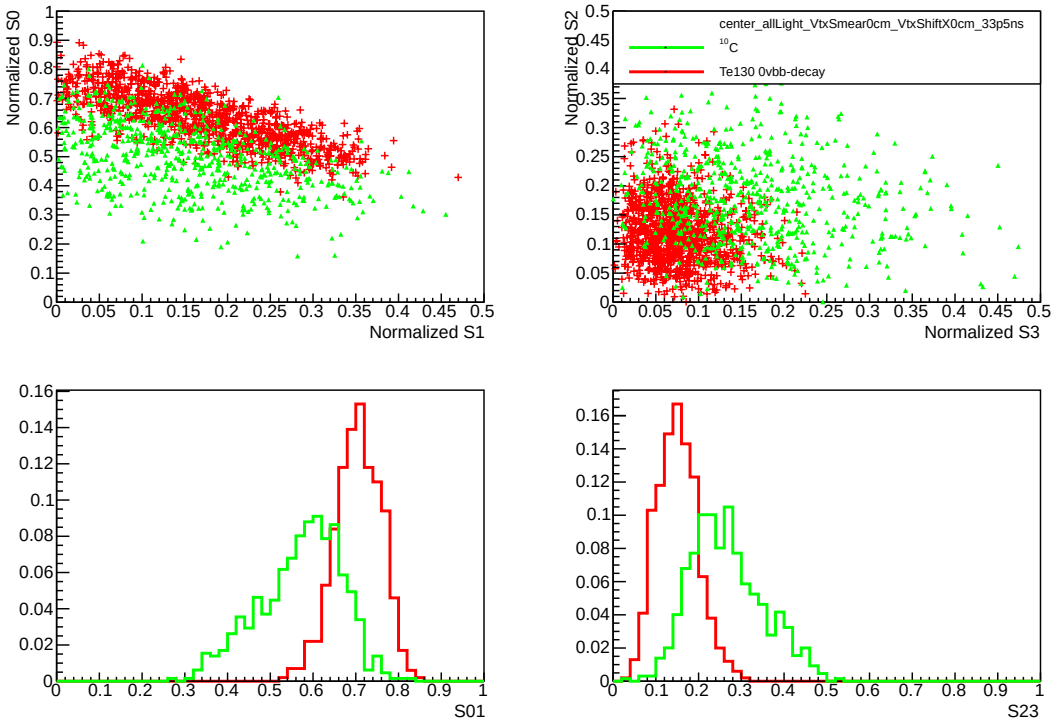

Figure 15: Spherical harmonics comparison between ^{130}Te $0\nu\beta\beta$-decay signal (Q=2.529 MeV) (red) and ^{10}C solar neutrinos background (blue) for 1000 simulated events originated at the center of the sphere. ^{10}C with energy deposition between 2.1 MeV and 2.9 MeV are considered. Perfect vertex reconstruction - true vertex position is used. Time cut of 33.5 ns on the photon arrival time is applied. (Top left) S_0 versus S_1 scatter plot. (Top right) S_2 versus S_3 scatter plot. (Bottom left) Distribution of the S_{01}^{C10} variable calculated for signal (red) and background (green). (Bottom right) Distribution of the S_{23}^{C10} variable calculated for signal (red) and background (green).

References

[1] C. Aberle et al. JINST 9 P06012.

[2] A good ref to SNO+ backgrounds description.